

Available online at www.sciencedirect.com

Energy Procedia 1 (2009) 2301–2306

**Energy
Procedia**www.elsevier.com/locate/procedia

GHGT-9

Detection of CO₂ leakage by eddy covariance during the ZERT project's CO₂ release experiments

Jennifer L. Lewicki^{a*}, George E. Hilley^b, Marc L. Fischer^c, Lehua Pan^a, Curtis M. Oldenburg^a, Laura Dobeck^d, Lee Spangler^d

^aEarth Sciences Division, Ernest Orlando Lawrence Berkeley National Laboratory, Berkeley, CA 94720, USA

^bDepartment of Geological and Environmental Sciences, Stanford University, Stanford, CA 94305 USA

^cEnvironmental Energy Technology Division, Ernest Orlando Lawrence Berkeley National Laboratory, Berkeley, CA 94720, USA

^dDepartment of Chemistry and Biochemistry, Montana State University, Bozeman, MT 59717 USA

Abstract

Carbon dioxide was released from a shallow horizontal well for ten days at 0.1 t d⁻¹ (Release 1) and for seven days at 0.3 t d⁻¹ (Release 2) during Summer 2007. Net CO₂ fluxes (F_c) were continuously monitored by eddy covariance during the summers of 2006 and 2007. To improve leakage detection ability, we removed ecosystem fluxes correlated with changes in soil temperature and light intensity from F_c . The Release 2 leakage signal was enhanced in a time series of upper 95th percentile residual F_c , while the Release 1 signal fell within the variability of unmodeled processes.

© 2009 Elsevier Ltd. Open access under [CC BY-NC-ND license](http://creativecommons.org/licenses/by-nc-nd/3.0/).

Keywords: Eddy covariance; Carbon dioxide flux; Geologic carbon storage monitoring; Leakage

1. Introduction

Eddy covariance (EC) is a micrometeorological technique commonly used to measure the flux of CO₂ (and other trace gases and heat) across the interface between a plant canopy and the atmosphere [e.g., Baldocchi, 1]. Because EC offers the benefit of a CO₂ flux measurement that (1) is automated, (2) does not interfere with the ground surface, and (3) is averaged over both time and space, with the spatial scale significantly larger (m²-km²) than that of many other ground-based methods, it has been proposed for use in monitoring programs at geologic carbon sequestration (GCS) sites [e.g., Miles et al., 2; Oldenburg et al., 3; Leuning et al., 4]. Importantly, however, the theory that underlies the EC method assumes that the surface the measurement is made over is horizontal and homogeneous and that atmospheric conditions at the time of the measurement are steady. Furthermore, the ability

* Corresponding author. Tel.: +001-510-495-2818; fax: +001-510-486-5686.

E-mail address: jllewicki@lbl.gov.

of EC to detect potentially small CO₂ leakage signals within the large background variability of ecological fluxes is largely untested.

The Zero Emissions Research and Technology (ZERT) shallow release facility at Montana State University provides the opportunity to conduct controlled releases of CO₂ from point and line sources, and test the ability of different CO₂ measurement technologies to detect, locate, and quantify CO₂ leakage within the near-surface environment [Lewicki et al., 5]. Two releases of CO₂ were carried out at different rates from a shallow horizontal well in July and August 2007. The spatio-temporal evolution of the surface leakage flux signals was characterized by repeated accumulation chamber measurements [Lewicki et al., 5]. Lewicki et al. [6] monitored net CO₂ fluxes using EC during the summers of 2006 and 2007. We present EC CO₂ flux measurements and apply a filtering method that removes the background ecosystem CO₂ fluxes correlated with variations in soil temperature and light intensity to enhance leakage detection ability. We show that EC is a promising technique for use in monitoring programs at GCS sites.

2. ZERT CO₂ Release Facility and Experiments

The CO₂ release experiments were conducted at the ZERT shallow release facility on the property of Montana State University in Bozeman, MT. The study site was a ~0.12 km² nearly flat agricultural field, with vegetation composed primarily of prairie grasses, alfalfa, and Canadian thistle. The field was mowed/hayed on 11 July 2006 and 22 June 2007. A ~30 cm-thick clay topsoil here overlies a ~20 cm-thick clayey silt layer, which overlies an alluvial sandy cobble. A N45E-trending horizontal well was installed in the field with a 73-m long central slotted (perforated) section and 15- and 12-m long unslotted sections on its sloping NE and SW ends, respectively. The slotted section was located at ~1.3-2.5 m depth, sub-water table, within the alluvial sandy cobble and was divided into six ~12-m long zones separated by 0.4-m wide inflatable packers. From 9-18 July 2007, 0.1 tonnes of CO₂ per day (t d⁻¹) were released from the well (hereafter referred to as Release 1). From 3-10 August 2007, 0.3 t CO₂ d⁻¹ were released (hereafter referred to as Release 2). The lower rate was selected based on numerical simulations to provide a challenging detection problem while still ensuring that injected CO₂ would reach the ground surface and the higher rate was selected to obtain a larger surface flux for demonstration purposes.

Lewicki et al. [5] measured soil CO₂ fluxes using the accumulation chamber method on a grid repeatedly on a daily basis, which characterized the spatio-temporal evolution of surface leakage during Releases 1 and 2. Surface CO₂ leakage was typically focused within ~5 m of the well trace at 5-6 points aligned along the surface well trace (Figure 1). The maximum soil CO₂ flux measured during Release 1 was high (~1600 g m⁻² d⁻¹), relative to background ecosystem respiration fluxes. However, the total CO₂ release rate of 0.1 t d⁻¹ was of similar magnitude as background ecosystem respiration flux integrated over the relatively small grid area (7.7 × 10⁻³ m²) [Lewicki et al., 5]. The maximum soil CO₂ flux measured during Release 2 was ~6000 g m⁻² d⁻¹, while the total CO₂ release rate of 0.3 t d⁻¹ was ~three times that of background ecosystem respiration flux integrated over the grid area at that time.

3. Methods

An EC station was deployed near the center of the field from 8 June to 4 September 2006 and then 27 m northwest of the release well from 28 May to 4 September 2007 (Figure 1a) [Lewicki et al., 6]. The EC station location took advantage of east-southeasterly prevailing winds, which frequently situated the EC station downwind of the horizontal well. The station was composed of fast- and slow-response subsystems. The fast-response subsystem included two sensors used to measure the variables necessary to calculate turbulent fluxes of CO₂, H₂O, heat, and momentum. A Gill-Solent WindMaster Pro sonic three-dimensional anemometer/thermometer (Gill Instruments, Ltd) measured wind speeds in three directions and sonic temperature at 10 Hz. A LI-COR 7500 open-path CO₂-H₂O infrared gas analyzer (LI-COR, Inc) measured CO₂ and water vapor densities at 10 Hz. Both sensors were mounted atop a tripod tower at 3.2 m height from 8 June to 4 September 2006, 3.0 m height from 28 May to 18 July 2007, and 2.8 m height from 19 July to 4 September 2007. The slow-response subsystem included sensors associated with a second tripod tower that measured auxiliary meteorological and soil physical parameters. In particular, photosynthetically active radiation (*PAR*) was measured with a LI-COR LI-190SA quantum sensor and soil temperature profiles (10, 20, and 30 cm depth) were measured at two locations with thermocouples.

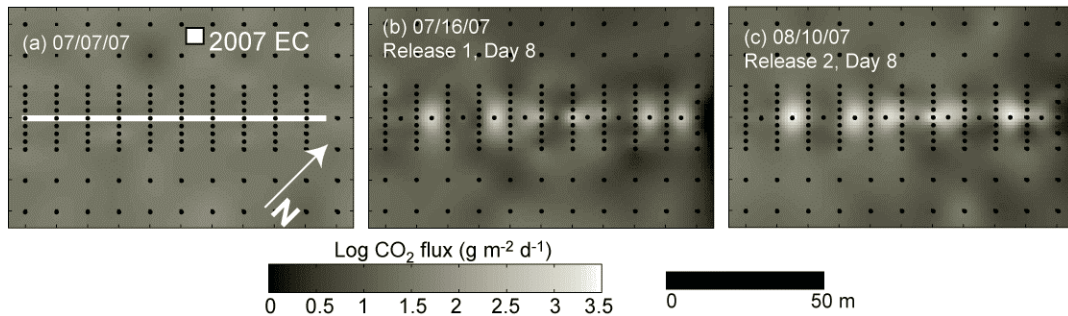


Figure 1. Image maps of log soil CO₂ flux, measured using the accumulation chamber method (a) prior to Release 1 on 07/07/07, (b) on Day 8 of Release 1, and (c) on Day 8 of Release 2. Black dots show measurement locations. White line and square on (a) show approximate locations of surface trace of horizontal well and 2007 EC station, respectively.

Net CO₂ flux (F_c) was calculated as the temporal covariance of CO₂ density (c) and vertical wind velocity (w):

$$F_c = \overline{w'c'}, \quad (1)$$

where the overbar denotes time averaging and primes denote fluctuations in w and c relative to their mean values. Fluxes were calculated for 30-minute periods. For each half-hour of data, the mean lateral (\bar{v}) and then the mean vertical (\bar{w}) wind velocities were rotated to zero [Kaimal and Finnigan, 7]. The Webb correction for the effects of fluctuation in heat and water vapor on the density of air [Webb et al., 8] was applied. Raw signals from the infrared gas analyzer and sonic anemometer were evaluated for spikes and all points more than ten standard deviations away from a 60 s moving average were removed from the data. Turbulent fluxes measured during the nighttime under low turbulent conditions can be systematically underestimated [e.g., Aubinet et al., 9; Massman and Lee, 10]. We therefore assessed the relationship between nighttime F_c and friction velocity (u_*) and discarded nighttime F_c data corresponding to $u_* \leq 0.15 \text{ m s}^{-1}$. F_c data were tested for stationarity according to Foken and Wichura [11] and non-stationary data were discarded. The reader is referred to Lewicki et al. [6] for more details on EC measurements.

4. Results

The mean and standard deviation of the 2006 half-hour F_c time series were -12.4 and $28.1 \text{ g m}^{-2} \text{ d}^{-1}$, respectively, whereas the mean and standard deviation of the 2007 half-hour F_c time series were -12.0 and $28.1 \text{ g m}^{-2} \text{ d}^{-1}$, respectively [Lewicki et al., 6]. Figure 2 shows the average daily nighttime and daytime F_c for the summers of 2006 and 2007. Average nighttime F_c were always positive, while average daytime F_c were typically negative, with the exception of the time periods immediately following mowing of the field. The field was a net sink for CO₂ prior to mowing in 2006 and 2007. The field became a net source for CO₂ when plant leaf area and photosynthetic uptake were decreased during mowing. Daytime CO₂ uptake then gradually increased through late July/early August, thereafter remaining relatively constant for the remainder of the 2006 and 2007 observation periods. CO₂ leakage during Release 1 was not possible to detect within the 2007 F_c time series (Figure 2b). However, average daytime and nighttime F_c measured during Release 2 shifted upwards, relative to the weeks prior to and following the release (Figure 2b).

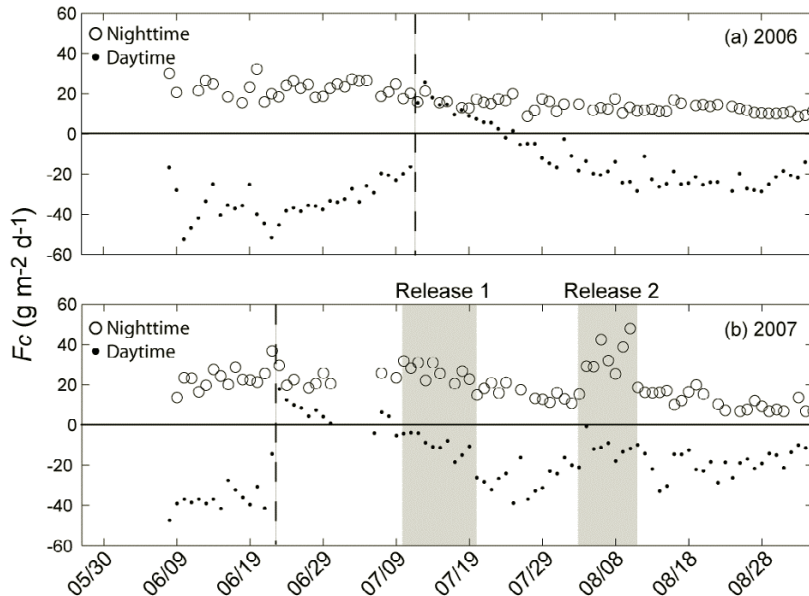


Figure 2. Average nighttime (open circles) and daytime (black dots) F_c measured in (a) 2006 and (b) 2007. Vertical dashed lines and gray zones indicate timing of mowing and CO_2 releases, respectively.

Because ecosystem fluxes are highly variable, they can mask CO_2 leakage signals similar to those studied here. Estimation and removal of the contribution of net ecosystem exchange (NEE) from the total measured flux, F_c may therefore improve our ability to detect leakage. NEE can be separated into photosynthetic uptake by the plant canopy and ecosystem respiration from plants and soil (R_{eco}). Although these constituent fluxes are influenced by many factors, intensity of light and soil temperature (T_{soil}) are strong drivers of short time-scale variations in plant photosynthetic uptake and R_{eco} , respectively. Consequently, empirically derived relationships between F_c and PAR and T_{soil} have been used to decompose F_c into R_{eco} and photosynthetic flux components and gap-fill F_c time series [e.g., Aubinet et al., 9; Falge et al., 12; Fischer et al., 13]. Here, the ecological F_c signals correlated with changes in PAR and T_{soil} were removed from the 2006 and 2007 F_c time series [Lewicki et al., 6]. The following relationship was used to describe NEE in terms of photosynthetic uptake and respiratory release of CO_2 :

$$NEE = -\left(\frac{F_{max}\alpha PAR}{\alpha PAR + F_{max}}\right) + b_0 \exp(bT_{soil}), \quad (2)$$

where F_{max} is the maximum CO_2 flux at infinite light, α is the apparent quantum yield, and b and b_0 are empirical coefficients. The first and second terms on the right side of equation (2) describe the photosynthetic uptake and R_{eco} components of NEE , respectively. Using nonlinear optimization methods, equation (2) was fit to half-hour F_c , T_{soil} (20 cm depth), and PAR data for three-day moving (half-hour time step) windows through the 2006 and 2007 measurement periods to estimate α , F_{max} , b and b_0 parameters for the center point in the moving window. Predicted values of NEE were then calculated for the center point based on measured F_c , T_{soil} , and PAR values and best-fit parameters. At least 20 data points were required within the three-day moving window for estimation of α , F_{max} , b and b_0 . Otherwise, a gap occurred for predicted NEE . A simple “ecological flux filter” was then applied by subtracting predicted NEE from measured F_c to yield residual F_c (F_{cr}). F_{cr} values represent fluxes that may result from background instrument noise, unmodeled natural processes, and CO_2 leakage. The mean and standard

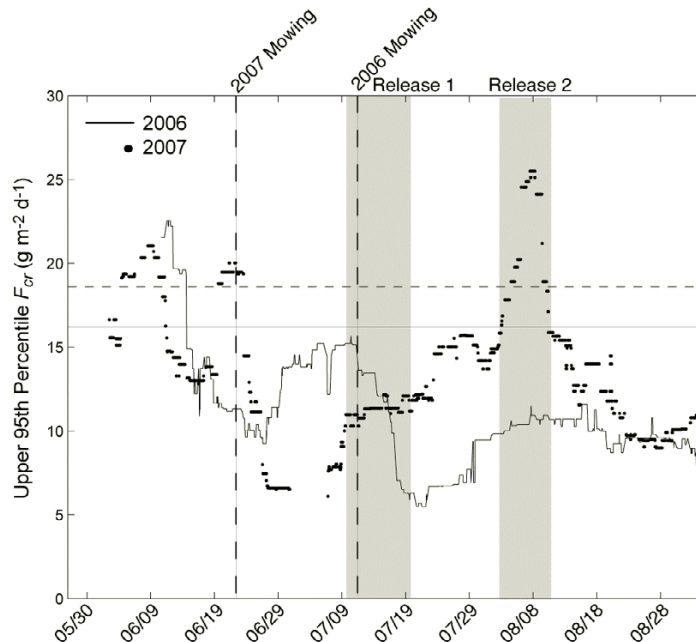


Figure 3. Upper 95th percentile F_{cr} for 2006 (line) and 2007 (black dots). Vertical dashed lines and gray zones indicate timing of mowing and CO₂ releases, respectively. Horizontal solid and dashed lines are 95th percentile residual flux for an exhaustively sampled stationary Gaussian distributions with mean and standard deviation = 0 and 8.1 g m⁻² d⁻¹ (2006) and 0 and 9.3 g m⁻² d⁻¹ (2007), respectively.

deviation of the 2006 F_{cr} time series were 0.0 and 8.1 g m⁻² d⁻¹, respectively, and the mean and standard deviation of the 2007 F_{cr} time series were -0.1 and 9.3 g m⁻² d⁻¹, respectively [Lewicki et al., 6].

The distribution of CO₂ leakage fluxes should have a positive mean. Therefore, to distinguish values that could be representative of leakage, we calculated the upper 95th percentile F_{cr} for the center point of a seven-day moving window (half-hour time step) through the 2006 and 2007 F_{cr} time series (Figure 3). For a stationary Gaussian distribution, the upper 95th percentile F_{cr} is two standard deviations above the mean. Assuming stationarity and that the mean is zero for 2006 and 2007 F_{cr} distributions, the upper 95th percentile F_{cr} for these distributions = 16.2 and 18.6 g m⁻² d⁻¹, respectively (dashed horizontal lines on Figure 3). Upper 95th percentile F_{cr} measured in 2006 and 2007 typically lay close to or below these thresholds, including those near the timing of mowing of the field. Exceptions to this pattern included several high-frequency increases in upper 95th percentile F_{cr} near the beginning of the time series, and the relatively high values sustained over multiple days during Release 2. Upper 95th percentile F_{cr} observed during Release 1 fell within the variability of background values.

5. Discussion and Conclusions

We tested the ability of EC to detect surface CO₂ leakage associated with two shallow subsurface CO₂ releases within a background ecosystem. The two release experiments provided a challenging leakage detection problem for EC due to the relatively small spatial extent of the leakage signals (Figure 1). Also, the surface CO₂ leakage rate estimated based on accumulation chamber measurements during Release 1 was comparable to the background ecosystem respiration flux integrated over the relatively small measurement grid area [Lewicki et al., 5]. Measurements of F_c in 2006 and 2007 prior to and following Releases 1 and 2 yielded a background summertime time series with which to compare measurements made during the releases. Average daytime and nighttime F_c measured during Release 1 were difficult to discern from background values, whereas those measured during Release 2 showed a positive shift upwards, relative to values measured during the weeks prior to and following the

release (Figure 2). Application of a simple filter that removed photosynthetic uptake and ecosystem respiration fluxes correlated with changes in PAR and T_{soil} , respectively, reduced the variability and negative bias observed in 2006 and 2007 half-hour F_c time series [Lewicki et al., 6]. Also, the leakage signal associated with Release 2 was enhanced and clearly detectable in the upper 95th percentile F_{cr} time series, whereas the Release 1 leakage signal remained undetectable. Future filtering methods should remove variations in F_c associated with currently unaccounted for natural processes (e.g., fluctuations associated with changes in vapor pressure deficit and soil moisture) and instrument noise to further improve EC detection of very small leakage signals.

Once a leakage signal is detected, EC has the potential to locate and quantify the leak. For example, Lewicki et al. [6] used a radial plot of F_{cr} as a function of mean horizontal wind direction to show that anomalously high F_{cr} values were typically measured during Release 2 when the EC station was downwind of the horizontal well. If the location of the leakage source were unknown, such a plot, in concert with footprint modeling of the EC flux source area, could assist in location of the leakage signal. Furthermore, Lewicki et al. [6] inverted F_{cr} measurements and corresponding footprint functions using a least-squares approach to model the spatial distribution of surface CO_2 fluxes during Release 2. Their inversion results roughly located the CO_2 leak, whereas the limited number of F_{cr} measurements available for use in the inversion did not provide model resolution sufficient to quantify the leakage rate [Lewicki et al., 6]. Simultaneous and repeated measurement of a given leakage signal by multiple EC stations with different flux source areas could improve leakage quantification. Given careful site-specific experiment design, EC is a promising tool for use in GCS monitoring programs.

Acknowledgements. We thank K. Gullickson for assistance in the field. This work was funded by the ZERT Project, Assistant Secretary for Fossil Energy, Office of Sequestration, Hydrogen, and Clean Coal Fuels, NETL, of the U.S. Dept. of Energy under Contract No. DE-AC02-05CH11231.

References

1. D.D. Baldocchi, (2003) Assessing the eddy covariance technique for evaluating carbon dioxide exchange rates of ecosystems: past, present, and future, *Global Change Biol.* 9 479.
2. N. Miles, K. Davis, and J. Wyngaard, (2005) Detecting leaks from CO_2 reservoirs using micrometeorological methods; In: *Carbon Dioxide Capture for Storage in Deep Geologic Formations-Results From the CO_2 Capture Project* [S. M. Benson] 1031–1044, Elsevier Science, London, U.K.
3. C.M. Oldenburg, J.L. Lewicki, and R.P. Hepple (2003) Near-surface monitoring strategies for carbon dioxide storage verification, *Lawrence Berkeley National Laboratory Report LBNL-54089* (2003).
4. R. Leuning, D. Etheridge, and B. Dunge, *Int. J. Greenhouse Gas Control* 2 (2008) 401.
5. J.L. Lewicki, C.M. Oldenburg, L. Dobeck, and L. Spangler (2007) Surface CO_2 leakage during two shallow subsurface CO_2 releases, *Geophys. Res. Lett.* 34 L24402, doi:10.1029/2007GL032047.
6. J.L. Lewicki, G.E. Hilley, M.L. Fischer, L. Pan, C.M. Oldenburg, L. Dobeck, and L. Spangler (2008) Eddy covariance observations of surface leakage during shallow subsurface CO_2 releases, *J. Geophys. Res.* in review.
7. J.C. Kaimal and J.J. Finnigan, (1994) *Atmospheric Boundary Layer Flows: Their Structure and Measurement*, Oxford University Press, Oxford, U.K.
8. E.K. Webb, G.I. Pearman, and R. Leuning (1980) Correction of flux measurements for density effects due to heat and water vapour transfer, *Quart. J. Royal Meteorol. Soc.*, 106, 85–100.
9. M. Aubinet, A. Grelle, A. Ibrom et al. (2000) Estimates of the annual net carbon and water exchange of European forests: the EUROFLUX methodology, *Advan. Ecol. Res.*, 30, 113–175.
10. W.J. Massman and X. Lee (2002) Eddy covariance flux corrections and uncertainties in long-term studies of carbon and energy exchanges, *Agric. For. Meteorol.*, 113, 121–144.
11. T. Foken and B. Wichura Foken (1996) Tools for quality assessment of surface-based flux measurements, *Agric. For. Meteorol.*, 78, 83–105.
12. E. Falge, D.D. Baldocchi, R.J. Olson, et al. (2001) Gap filling strategies for defensible annual sums of net ecosystems exchange, *Agric. For. Meteorol.*, 107, 43–69.
13. M.L. Fischer, D.P. Billesbach, J.A. Berry, R.J. Riley, and M.S. Torn (2007) Spatiotemporal variations in growing season exchanges of CO_2 , H_2O , and sensible heat in agricultural fields of the southern Great Plains, *Earth Interact.*, 11, 1–21.